Conditioning Effects on $La_{1-x}Sr_xMnO_3$-Yttria Stabilized Zirconia Electrodes for Thin-Film Solid Oxide Fuel Cells

You-Kee Lee[a,*], Jung-Yeul Kim[a], Young-Ki Lee[a], Insoo Kim[b], Hee-Soo Moon[c], Jong-Wan Park[c], Craig P. Jacobson[d] and Steven J. Visco[d]

[a]*Division of Information & Communication Engineering and Science and Engineering Research Institute (SERI), Uiduk University, Kyongju 780-713, Korea*

[b]*Department of Metallurgical Engineering, Dong-A University, Pusan 604-714, Korea*

[c]*Division of Materials Science & Engineering, Hanyang University, Seoul 133-791, Korea*

[d]*Materials Sciences Division, Lawrence Berkeley National Laboratory, CA 94720, USA*

Abstract

Composite cathodes of 50/50 vol% LSM-YSZ ($La_{1-x}Sr_xMnO_3$-yttria stabilized zirconia) were deposited onto dense YSZ electrolytes by a colloidal deposition technique. The cathode characteristics were then examined by scanning electron microscopy (SEM) and studied by ac impedance spectroscopy (IS). Conditioning effects of the LSM-YSZ cathodes were seen, and remedies for these effects were proposed for improving the performance of a solid oxide fuel cell (SOFC). LSM surface contamination and modification, cathode bonding to the YSZ electrolyte, changing Pt electrode and bonding paste, and curvature of sintered YSZ electrolytes led to some changes in microstructure and variability in cell performances. Much of the variability could be eliminated by using only one batch of Pt paste, using flat and sanded YSZ plates as well as consistent processing procedures. Reproducible impedance spectra were obtained by using the improved cell configurations. Typical IS spectra measured for an (air)LSM-YSZ/YSZ/LSM-YSZ(air) cell at 900℃ showed two depressed arcs. The impedance characteristics of the LSM-

YSZ cathodes were also affected by experimental conditions such as surface modification of the LSM by Ni or Sr, cathode compositions and applied current.

Keywords: Composite cathodes; Colloidal deposition technique; Conditioning effects; Impedance characteristics

*Corresponding author. Fax: +82-54-760-1504

E-mail address: leeyk@mail.uiduk.ac.kr

1. Introduction

In recent years several groups worldwide have been involved in the development of solid oxide fuel cells (SOFCs) capable of delivering high power at reduced temperatures, and remarkable progress has been made in developing reduced temperature SOFCs. The approaches generally fall into two categories: the use of materials with substantially higher conductivity and/or fabrication of SOFCs using thin-film electrolyte membranes. Several methods for depositing thin-film onto porous SOFC electrodes/substrates have attracted widespread attention because the electrolyte ohmic loss became negligibly small as electrolyte thickness was reduced [1-6]. A high-performance, planar thin-film SOFC fabricated by a colloidal deposition of YSZ on porous electrode, showing excellent performance at 800 ^{0}C, was first reported by de Souza *et al.*[5]. Clearly, after the resistance of the electrolyte has been lowered to acceptable (or negligible) levels, the performance of the anode and, particularly, the cathode becomes the limiting factor to performance at temperature below 800℃.

$La_{1-x}Sr_xMnO_3$ (LSM) has been considered one of the most promising cathode materials for SOFC due to its the good performance [7]. At reduced temperatures (700-800℃), however, the related cathode overpotential remains significant in SOFCs. Therefore, it is desirable to decrease further the overpotential for the LSM cathode. In recent studies, improvement of electrochemical performance relative to the performance of the conventional LSM cathodes was observed for composite cathodes produced by mixing powders of YSZ and LSM. This result could be attributed to the contribution of the increased length of triple-phase boundaries (TPB) constituting the electrode/electrolyte/gas interface. It is clear that composite electrodes (*i.e.*, LSM-YSZ) perform much better than the single component electrodes (*i.e.*, LSM). However, there still remains controversy regarding the details of the electrode kinetics, since the experimental conditions (*i.e.*, chemical composition, grain/particle size distribution, microstructure, thickness, firing temperature, porosity, etc.) play an important role. Therefore,

more information is needed to understand the performance of thin-film SOFCs with LSM-YSZ composite electrodes at reduced temperatures.

In this study the electrochemical evaluation of a series of perovskite electrodes is presented. Specifically, composite cathodes with 50/50 vol% LSM-YSZ are evaluated for use in conventional and thin-film SOFCs.

2. Experimental

For the electrolytes, sintered 8 mol% YSZ pellets were used. YSZ powder supplied by Tosoh Co., Ltd. was pressed, and sintered in air at 1450℃ for 4 h, to form pellets of ca. 30 mm in diameter and ca. 0.6 mm in thickness with relative density of more than 95% of theoretical. The YSZ pellets developed a curvature, corresponding to an offset of about 3mm in their center. The curvature avoided contact with the alumina setter plates during subsequent firing of the sprayed-on electrodes.

Various $La_{1-x}Sr_xMnO_3$ (LSM) powders with $0 \leq x \leq 0.5$ were prepared by the glycine-nitrate combustion process [8], with a glycine/nitrate ratio of 0.5. These powders were subsequently calcined in air at 1200℃ for 4 h. The resulting LSM powders and YSZ powders, in a ratio 50/50 vol%, were milled for 1.5 h in acetone, using zirconia milling media. The LSM-YSZ cathode powders were dried, dispersed in isopropyl alcohol, and applied to a 1 cm x 1 cm masked- off area on the electrolyte plates to form the working electrodes, and fired at 1100℃ for 4 h. The Pt counter- and Pt reference-electrodes were deposited on the other side of the YSZ plates as a thin layer of Pt paste (Heraeus), and then fired at 950℃ for 0.5 h. The current collector was Pt mesh, fixed to the electrode surface by Pt paste. After firing at 950℃ for 0.5 h, the Pt mesh adhered well to the electrodes. The thickness of the working electrode (LSM-YSZ) was

measured the be about 10 μm by SEM. Cells with YSZ electrolyte sandwiched between two similar LSM-YSZ cathode materials were also prepared. Some of he LSM electrodes were further modified by application of Ni or Sr as a nitrate solutions in isopropyl alcohol.

Impedance spectroscopy was used to measure the resistivity of the LSM-YSZ cathodes layers, using a computer-controlled Solatron SI 1260 Impedance/Gain-Phase Analyzer in combination with a PAR Potentiostat/Galvanostat. Impedance spectra were taken in the frequency range of 0.1 Hz to 100 kHz, and the applied AC amplitude was set to 10 mV. Impedance spectra were also obtained for samples after heat-up or cool-down to the measurement temperature, either immediately or after a 24 hr delay.

3. Results and discussion

Figure 1 shows the impedance spectra of $La_{0..85}Sr_{0.15}MnO_3$-YSZ (LSM15-YSZ)/YSZ electrode, obtained after increasing or decreasing the temperature, to the measurement temperatures between 700 and 900^0C. In Fig 1, the numbers 1 and 2 refer to results after increasing and after decreasing the temperatures to the measurement temperature, respectively, followed by a 1 day delay. The numbers 3 and 4 refer to results after increasing and after decreasing the temperatures to the measurement temperature, respectively, without delay. These spectra clearly indicate that the interfacial impedance (or polarization resistance) is a strong function of operating temperature and temperature history. With increasing operating temperature the LSM15-YSZ cathode impedance decreases. The impedance spectra also evidence a difference between spectra obtained after increasing or after decreasing to the operating temperature. For an operating temperature of 900^0C, however, the conditioning is no longer noticeable. This conditioning of the cathode polarization (arc size) can be interpreted as resulting from the changes in oxygen vacancy concentrations, and hence the ionic conductivity, of the LSM-YSZ electrode [9-12]. Stable conditions for LSM-YSZ/YSZ cells are typically reached immediately at 900^0C, but may take several days for cells operating well below 900^0C. The impedance spectra

typically show an inductive response at frequencies above 1 MHz, originating from the Pt lead connections and the instrumentation.

Figure 2 shows the deconvolution of the impedance spectrum of an LSM15-YSZ cathode measured at 900^0C in air with the corresponding equivalent circuit, after subtraction of the inductive response. Deconvolution of the complex impedance spectrum was performed with Zplot and Zview (Scribner Associates Inc.) electrochemical impedance software, and appropriate parameters for the appropriate equivalent model circuit were determined. The impedance spectrum of the LSM-YSZ electrode shows two overlapping semicircles: the one at the high frequency side was due to charge transfer process; the other at the low frequency one can be attributed to mass transfer (or diffusion process) of the oxide ion [13-19]. Also, the spectrum shows that high frequency arc is much smaller than the low frequency arc. This result indicates that mass transfer (low frequency arc) is dominant in this LSM-YSZ cathode.

Figure 3 shows the impedance spectra obtained from LSM15-YSZ and LSM15 cathodes deposited on as-sintered YSZ surface and on sanded YSZ surface, exposed to air at 800^0C. The polarization resistance of both the LSM15-YSZ and LSM15 deposited on sanded YSZ surfaces typically decreased compared to those deposited on as-sintered YSZ surfaces. This result can be related to increasing the effective TPB length and removal of surface impurities. A sintered YSZ surface is generally smooth and glossy and contains surface impurities such as silica and alumina. Therefore, the surface treatment such as abrasion and etching is helpful to the creation of extra TPB in addition to the removal of surface impurities. If the impurities are present at the electrode/electrolyte triple phase boundary interface, then clearly they can restrict the flux of oxygen ions into the electrolyte. The removal of impurities, particularly silica, in YSZ electrolytes can thus decrease the electrode resistivity as well as the ionic resistivity of the YSZ electrolyte. The surface pretreatment also helped to increase the adhesion of electrode materials during further processing. Other researchers also have reported similar results [20,21].

In Fig. 3, the polarization resistance of LSM15-YSZ cathode is shown to be lower than that of LSM15. This result indicates that with addition of YSZ to the LSM15 electrode, spatial enlargement of the TPB length was realized so that the oxygen ion transfer step could be accelerated. It is also evident from Fig. 3 that the polarization resistance of LSM15-YSZ cathodes deposited on sanded YSZ surface is much reduced compared to that of LSM15. This result supports further that the polarization resistance of LSM15-YSZ cathode deposited on sanded YSZ surface is drastically decreased due to the combination of spatial enlargement of the TPB length and removal of the surface impurities as mentioned above.

Figure 4 shows the impedance spectra obtained from LSM15-YSZ and LSM15 with and without Ni- or Sr-nitrate modification. For LSM15-YSZ modified with Ni or Sr, the polarization resistance was much smaller than for LSM15-YSZ without Ni or Sr, whereas for the LSM15 with the Ni or Sr modification, the opposite result was obtained. This result is not clearly understood at present. Generally, the polarizability of SOFC electrodes is reduced by the presence of additional catalytically active elements. The effect is associated with an increasing rate of interface oxygen exchange at either electrode/gas or electrolyte/gas surfaces, with an increasing TPB activity, or with a combination of these factors. At the same time, we may postulate that substitution of manganese by diffusion and/or reaction of catalytic elements into the LSM15 can lead to a significant decrease in oxygen diffusivity, although it leads to an increase in the surface electrochemical activity of the LSM15 cathode. A full analysis is the subject of future work.

Figure 5 shows typical impedance spectra of LSM-YSZ/YSZ/LSM-YSZ cells with different LSM-YSZ electrode compositions on YSZ electrolyte, in air, at 900^0C. The spectra of the cathodic side half-cell and anodic side half-cell were not from the same half-cells because of the geometrical asymmetry (curved surface) of the two half-cells. These spectra clearly indicate that the interfacial impedance is a strong function of the composition of electrode materials and the geometry of the electrolytes. These spectra don't show a clear dependency of impedance on the Sr-content in LSM-YSZ. Therefore, at this time we can postulate that the compositional

effects of the LSM in LSM-YSZ electrode can be readily overwhelmed by the quality of the bonding of the YSZ in electrode to the YSZ in the electrolyte or by the effect of the vol% of YSZ in the electrode. This will be examined in more detail in a future study.

Figure 6 shows impedance spectra obtained from LSM15-YSZ/YSZ/Pt cells with two different types of Pt anodes ((a) Pt-1 and (b) Pt-2). The two Pt pastes were also used to affix the Pt-mesh current collectors to the electrodes. These spectra of anodic side half-cell clearly indicate that the interfacial impedance is a strong function of the formulation of the Pt pastes, and the microstructures of the resulting electrode. Therefore, use of the only one batch Pt paste is advisable for acquisition of consistent data.

Figure 7 shows the impedance spectra of a LSM-YSZ/YSZ/Pt cell with LSM15-YSZ cathodes deposited on the curved YSZ surfaces, in air, at 900℃. The LSM-YSZ cathode and Pt anode deposited on the concave side of the YSZ plates showed a lower resistivity than those for convex side, while the LSM-YSZ cathode deposited on the concave side in turn showed higher resistivity compared to that of a flat YSZ plate. These results are most likely caused by concentration polarization due to variations in the electrode/electrolyte contact area, and to changes in the TPB length, as shown in SEM images of Fig. 8. Therefore, the use of electrolyte with a flat surface is advisable for fabrication of high performance cell.

Figure 8 shows the cross-section SEM photographs of three LSM-YSZ cathode layers. The electrode/electrolyte contact for convex side in the LSM-YSZ electrode appears to be much worse than for the concave or the flat side.

Figure 9 shows impedance spectra of LSM-YSZ cathodes before and after passing current. Measurements were taken at 900^0C, (a) before passing current, (b) 4 min after passing a current of 1 A/cm^2 for 24 h, and (c) 24 h after passing a current of 1 A/cm^2 for 24 h. For the impedances measured 4 min after switching off the current, a decrease of the electrode resistance was observed for a cells with a cathode composition of $LaMnO_3$-YSZ, $La_{0.9}Sr_{0.1}MnO_3$-YSZ, and

$La_{0..85}Sr_{0.15}MnO_3$-YSZ , compared to before current passage. In contrast, the impedances measured 24 h after switching off the current, showed a drastic increase of the electrode resistance for all cells, with exception of the cell with a $La_{0..85}Sr_{0.15}MnO_3$-YSZ cathode. Therefore, $La_{0..85}Sr_{0.15}MnO_3$-YSZ is the cathode with relatively low electrode resistance before and after current passage, and can be regarded as the best performing cathode material in the present study.

Figure 10 and 11 show SEM photographs of $La_{0..85}Sr_{0.15}MnO_3$-YSZ (LSM15-YSZ) and $La_{0..80}Sr_{0.20}MnO_3$-YSZ (LSM20-YSZ) in LSM-YSZ/YSZ/LSM-YSZ cells before and after passing a current of 1 A/cm^2, respectively. The difference in the thickness of LSM-YSZ is due to the detachment of a part of LSM-YSZ upon removal of the Pt mesh current collector from LSM-YSZ/YSZ cell for SEM observation. In the present work, we were not able to detect any change in the microstructure on the cathodic side of LSM-YSZ specimens induced by current passage. In contrast, the SEM images clearly show that a noticeable reaction layer has occurred at the anodic side of the YSZ after current passage. It is possible that some components of the LSM-YSZ anode diffuse into the YSZ upon current passage. Also, the LSM15-YSZ anode morphology has changed significantly, whereas the cathode doesn't show a change in microstructure after current passage. The morphology changes resulted in higher electrode polarization in LSM15-YSZ anode after current passage for various electrode compositions.

4. Conclusions

The cathode resistivities of 50/50 vol% LSM-YSZ for use in conventional and thin-film SOFCs were investigated by the complex ac impedance measurement. The electrode impedance response was very sensitive to the fabrication procedures. Reproducible impedance spectra could be obtained by establishing consistent processing and testing conditions of the cell components. Improvement of electrochemical performance for LSM-YSZ cathode materials at reduced temperatures is most likely to come from engineering of electrolyte/electrode interface.

Acknowledgements

This work was performed in the Materials Sciences Division of the Lawrence Berkeley National Laboratory with funding from the U.S. Department of Energy through the National Energy Technology Laboratory. One of the authors, You-Kee Lee, wishes to thank KOSEF (Korea Science and Engineering Foundation) for a Post Doctoral Fellowship.

References

[1] J. P. P. Huijsmans, F. P. F. van Berkel, G. M. Christie, *J. Power Sources*, **71** (1998) 107.

[2] L. S. Wang and S. A. Barnett, *Solid State Ionics*, **61** (1993) 273.

[3] H. Fukunaga, M. Ihara, K. Sakaki and K. Yamada, *ibid*., 86-88 (1996) 1179.

[4] P. K. Srivastava, T. Quach, Y. Y. Duan, R. Donelson, S. P. Jiang, F. T. Ciacchi and S. P. S. Badwal, *ibid.*, **99** (1997) 311.

[5] S. de Souza, S. J. Visco and L. C. De Jonghe, *ibid.*, **98** (1997) 57.

[6] T. Ioroi, T. Hara, Y. Uchimoto, Z. Ogumi and Z. Takehara, *J. Electrochem. Soc*., **144** (1997) 1362.

[7] N. Q. Minh, *J. Am. Ceram. Soc*., **76** (1993) 563

[8] L. A. Chick, L. R. Pederson, G. D. Maupin, J. L. Bates, L. E. Thomas and G. J. Exarhos, *Mat. Lett.*, **10** (1990) 6.

[9] M. J. L. Østergård and M. Mogensen, *Electrochem. Acta*, **38** (1993) 2105.

[10] H. Y. Lee, W. S. Cho, S. M. Oh, H-D. Wiemhöfer and W. Göpel, *J. Electrochem. Soc.*, **142** (1995) 2659.

[11] Y. Jiang, S. Wang, Y. Zhang, J. Yan and W. Li, *ibid*., **145** (1998) 373.

[12] A. Hammouche, E. Siebert, A. Hammon, M. Kleitz and A. Caneiro, *ibid*., **138** (1991) 1212.

[13] A. Hahn and H. Landes, Proceedings 5th Intern. Symp. SOFC, Aachen, Germany, June 1997, U. Stimming, S. C. Singhal, H. Tagawa, W. Lehnert eds., p.595, The Electrochemical Society, Inc., Pennington, NJ.

[14] Y. Shibuya and H. Nagamoto, *ibid*., p.510.

[15] T. Ioroi, T. Hara, Y. Uchimoto, Z. Ogumi and Z. Takehara, *J. Electrochem. Soc.*, **145** (1998) 1999.

[16] E. Siebert, A. Hammouche and M. Kleitz, *Electrochem. Acta*, **40** (1995) 1741.

[17] M. J. L. Østergård, C. Clausen, C. Bagger and M. Mogensen, *ibid.*, **40** (1995) 1971.

[18] E. P. Murray, T. Tsai and S. A. Barnett, *1998 Fuel Cell Seminar Abstracts*, p.414.

[19] M. Juhl, S. Primdahl and M. Mogensen, *Proc. 17th Ris Intern. Symp. on Mat. Sci*., F. W. Poulsen, N. Bonanos, S. Linderoth, M. Mogensen and B. Zachau-Christiansen eds., Ris National Laboratory, Denmark, p.295 (1996).

[20] T. Tsai and S. A. Barnett, *J. Electrochem. Soc*., **145** (1998) 1696.

[21] J-M. Bae and B. C. H. Steele, *Solid State Ionics*, **106** (1998) 247.

Caption lists

Fig. 1 Evolution of the impedance spectra for a LSM15-YSZ cathode on YSZ measured at (a) 700℃, (b) 750℃, (c) 800℃, (d) 850℃ and (e) 900℃ in air. In each figure, the 1 and 2 represent measured plots under increasing and decreasing of temperature, respectively, within 1 day, and 3 and 4 without 1 day after first measurement.

Fig. 2 Deconvolution of the impedance spectrum of LSM15-YSZ cathode measured at 900℃ in air with the equivalent circuit after subtraction of the inductance (R_1: YSZ electrolyte resistance, R_2: charge transfer resistance, R_3: mass transfer resistance, C_2, C_3: distributed capacitances).

Fig. 3 Impedance spectra for the LSM15/YSZ and LSM15-YSZ/YSZ electrodes with different YSZ electrolyte surfaces at 800℃ in air; (a) LSM15 with as-sintered YSZ surface, (b) LSM15 with sanded YSZ surface, (c) LSM15-YSZ with as-sintered YSZ surface and (d) LSM15-YSZ with sanded YSZ surface.

Fig. 4 Impedance spectra for the LSM15/YSZ and LSM15-YSZ/YSZ electrodes with different catalytic interlayer at 800℃ in air; (a) LSM15 with no catalytic interlayer, (b) LSM15 with Ni-nitrate, (c) LSM15 with Sr-nitrate, (d) LSM15-YSZ with no catalytic interlayer, (e) LSM15-YSZ with Ni-nitrate and (f) LSM15-YSZ with Sr-nitrate.

Fig. 5 Impedance spectra for the LSM-YSZ/YSZ/LSM-YSZ cells under various cathode compositions at 900℃ in air; (a) $LaMnO_3$-YSZ, (b) $La_{0.9}Sr_{0.1}MnO_3$-YSZ, (c) $La_{0.85}Sr_{0.15}MnO_3$-

YSZ, (d) $La_{0.8}Sr_{0.2}MnO_3$-YSZ, (e) $La_{0.7}Sr_{0.3}MnO_3$-YSZ, (f) $La_{0.6}Sr_{0.4}MnO_3$-YSZ and (g) $La_{0.5}Sr_{0.5}MnO_3$-YSZ.

Fig. 6 Impedance spectra obtained from LSM15-YSZ/YSZ/Pt cells with two different types of Pt anodes ((a) Pt-1 and (b) Pt-2). The two Pt pastes also applied as an adhesive of current collector in two electrodes.

Fig. 7 Impedance spectra of LSM15-YSZ cathodes with different YSZ electrolyte geometry at 900℃ in air; (a) electrode deposited on convex YSZ surface, (b) electrode deposited on concave YSZ surface and (c) electrode deposited on flat YSZ surface.

Fig. 8 SEM photographs of a cross-sectional fracture surface of LSM15-YSZ electrodes on (a) convex, (b) concave and (c) flat YSZ plates.

Fig. 9 Impedance spectra of LSM-YSZ cathodes before and after passing a current of 1 A / ㎠. Measurements were taken at 900℃, (a) before, (b) 4 min after and (c) 24 h after passing a current of 1 A / ㎠ for 24 h.

Fig. 10 SEM photographs of a cross-sectional fracture surface of LSM15-YSZ electrodes before and after current passage; (a) cathodic side before current passage, (b) anodic side before current passage, (c) cathodic side after current passage and (d) anodic side after current passage.

Fig. 11 SEM photographs of a cross-sectional fracture surface of LSM20-YSZ electrodes before and after current passage; (a) cathodic side before current passage, (b) anodic side before current passage, (c) cathodic side after current passage and (d) anodic side after current passage.

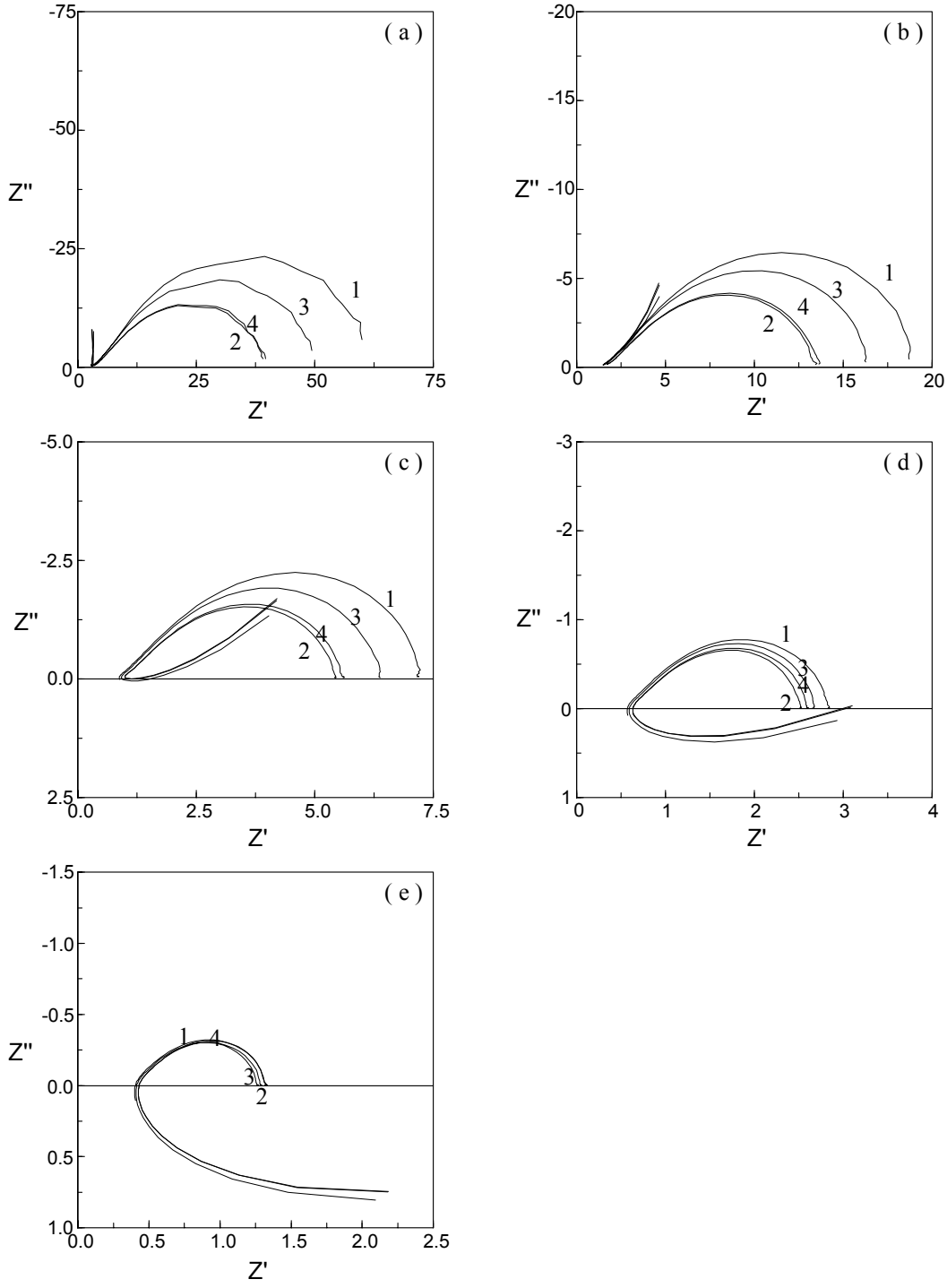

Fig. 1 Evolution of the impedance spectra for a LSM15-YSZ cathode on YSZ measured at (a) 700°C, (b) 750°C, (c) 800°C, (d) 850°C and (e) 900°C in air. In each figure, the 1 and 2 represent measured plots under increasing and decreasing of temperature, respectively, within 1 day, and 3 and 4 without 1 day after first measurement.

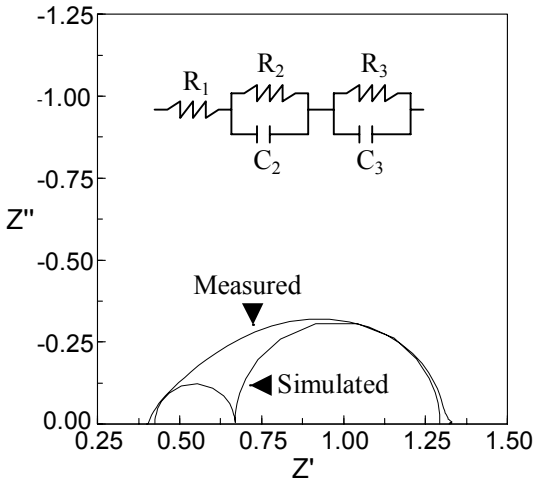

Fig. 2 Deconvolution of the impedance spectrum of LSM15-YSZ cathode measured at 900°C in air with the equivalent circuit after subtraction of the inductance (R_1: YSZ electrolyte resistance, R_2: charge transfer resistance, R_3: mass transfer resistance, C_2, C_3: distributed capacitances).

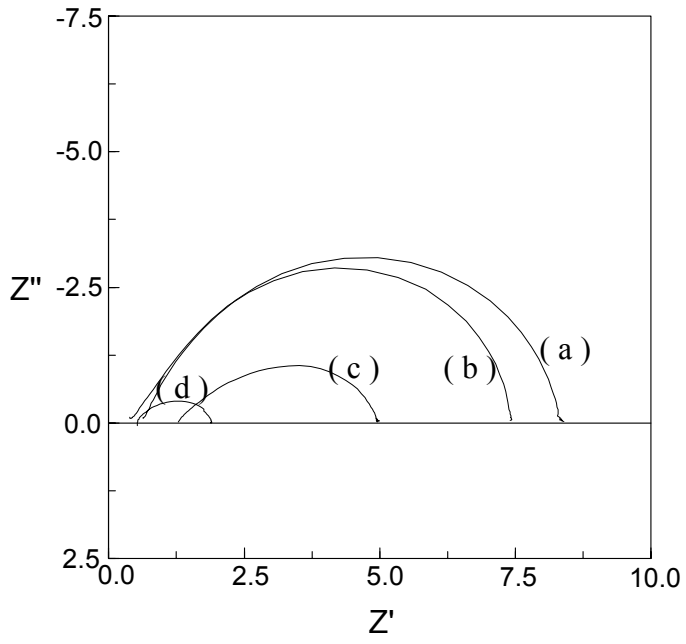

Fig. 3 Impedance spectra for the LSM15/YSZ and LSM15-YSZ/YSZ electrodes with different YSZ electrolyte surfaces at 800°C in air; (a) LSM15 with as-sintered YSZ surface, (b) LSM15 with sanded YSZ surface, (c) LSM15-YSZ with as-sintered YSZ surface and (d) LSM15-YSZ with sanded YSZ surface.

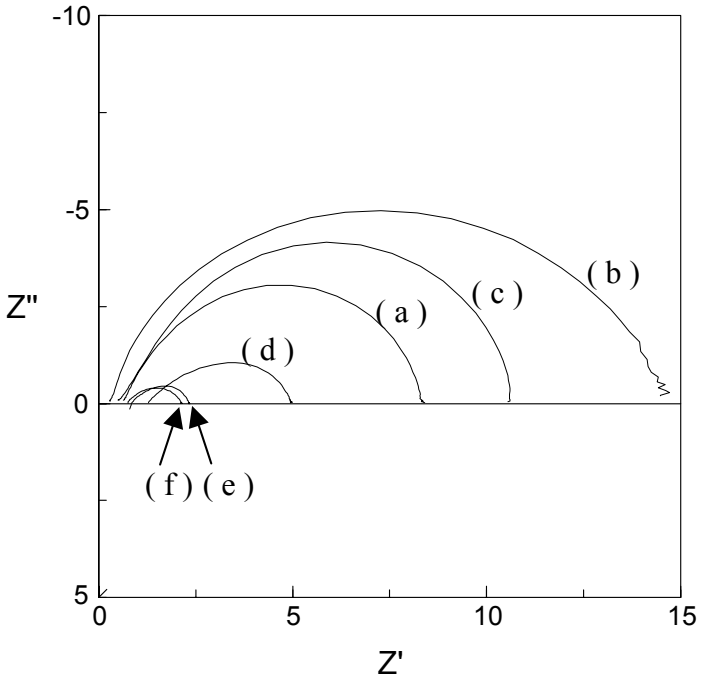

Fig. 4 Impedance spectra for the LSM15/YSZ and LSM15-YSZ/YSZ electrodes with different catalytic interlayer at 800°C in air; (a) LSM15 with no catalytic interlayer, (b) LSM15 with Ni-nitrate, (c) LSM15 with Sr-nitrate, (d) LSM15-YSZ with no catalytic interlayer, (e) LSM15-YSZ with Ni-nitrate and (f) LSM15-YSZ with Sr-nitrate.

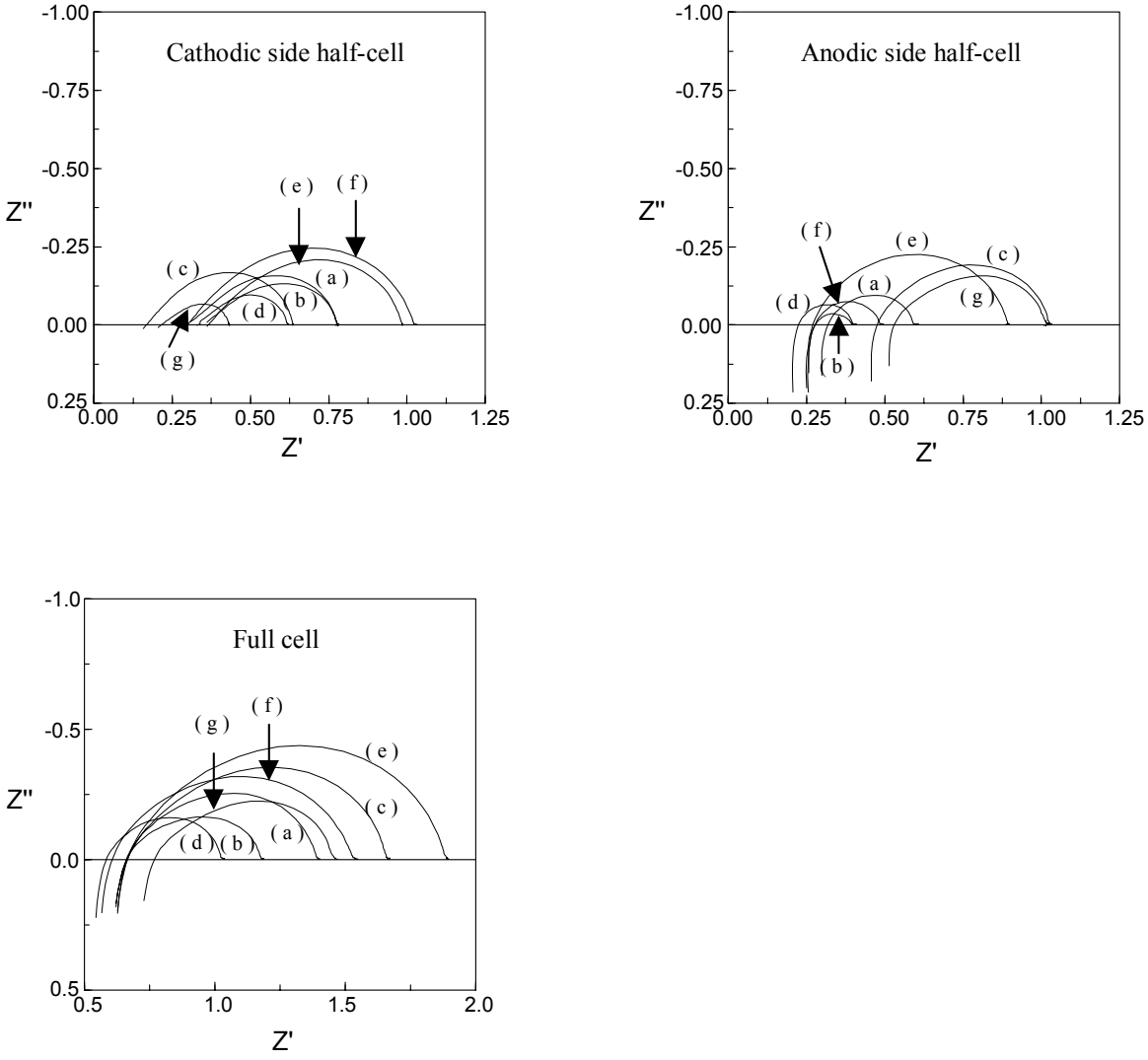

Fig. 5 Impedance spectra for the LSM-YSZ/YSZ/LSM-YSZ cells under various cathode compositions at 900°C in air; (a) $LaMnO_3$-YSZ, (b) $La_{0.9}Sr_{0.1}MnO_3$-YSZ, (c) $La_{0.85}Sr_{0.15}MnO_3$-YSZ, (d) $La_{0.8}Sr_{0.2}MnO_3$-YSZ, (e) $La_{0.7}Sr_{0.3}MnO_3$-YSZ, (f) $La_{0.6}Sr_{0.4}MnO_3$-YSZ and (g) $La_{0.5}Sr_{0.5}MnO_3$-YSZ.

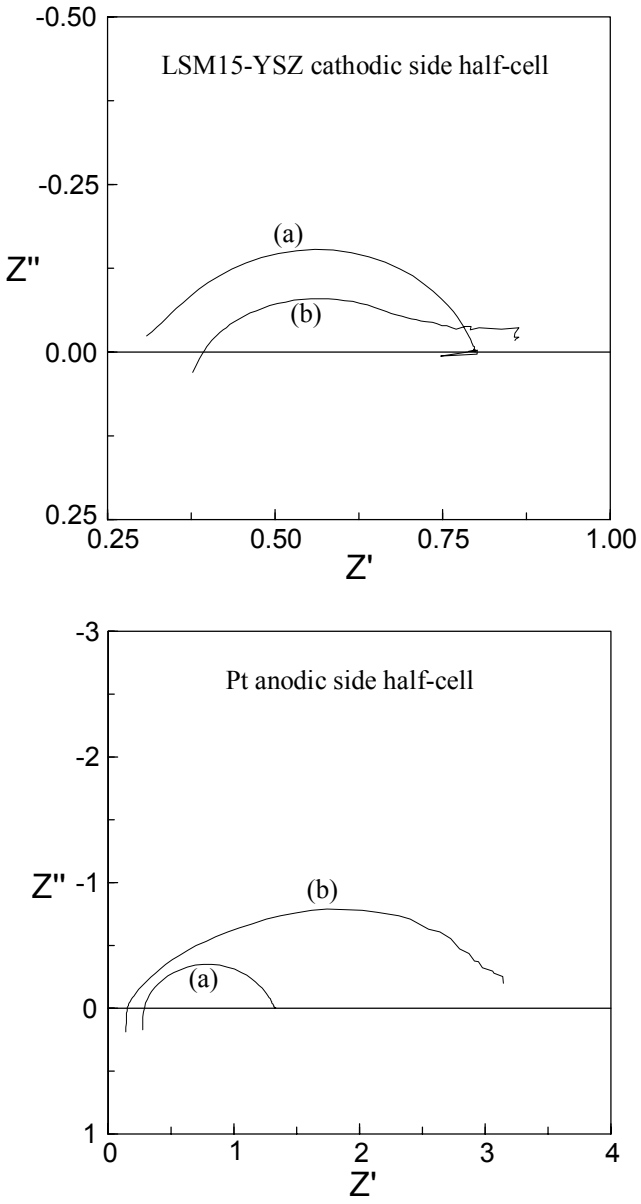

Fig. 6 Impedance spectra obtained from LSM15-YSZ/YSZ/Pt cells with two different types of Pt anodes ((a) Pt-1 and (b) Pt-2). The two Pt pastes also applied as an adhesive of current collector in two electrodes.

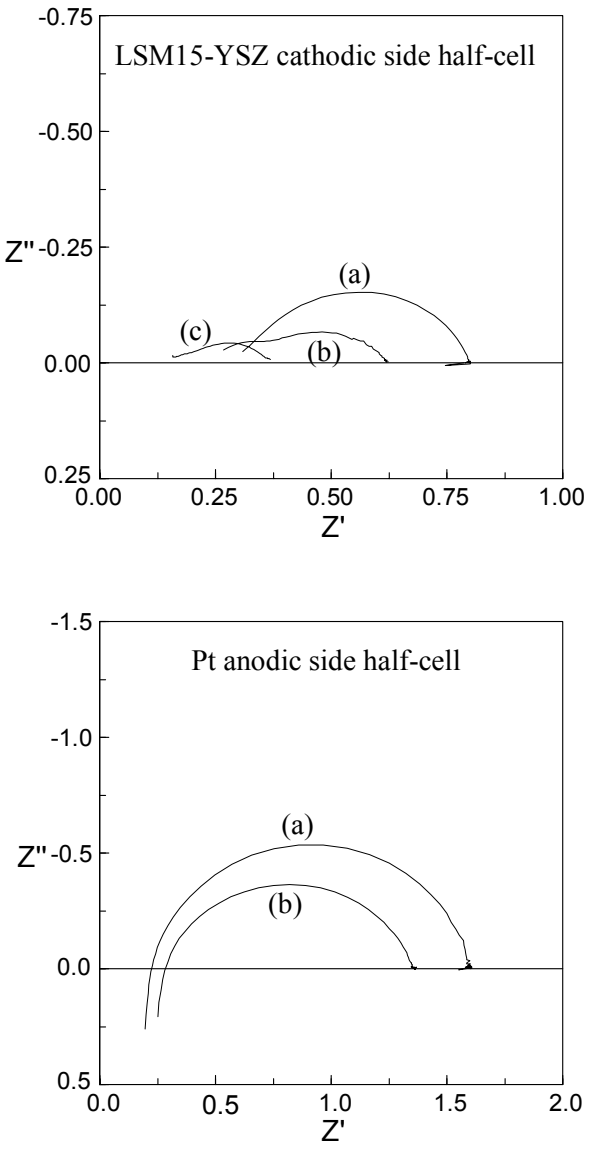

Fig. 7 Impedance spectra of LSM15-YSZ cathodes with Pt anode on curved YSZ surface at 900°C in air; (a) electrode deposited on convex YSZ surface, (b) electrode deposited on concave YSZ surface and (c) electrode deposited on flat YSZ surface.

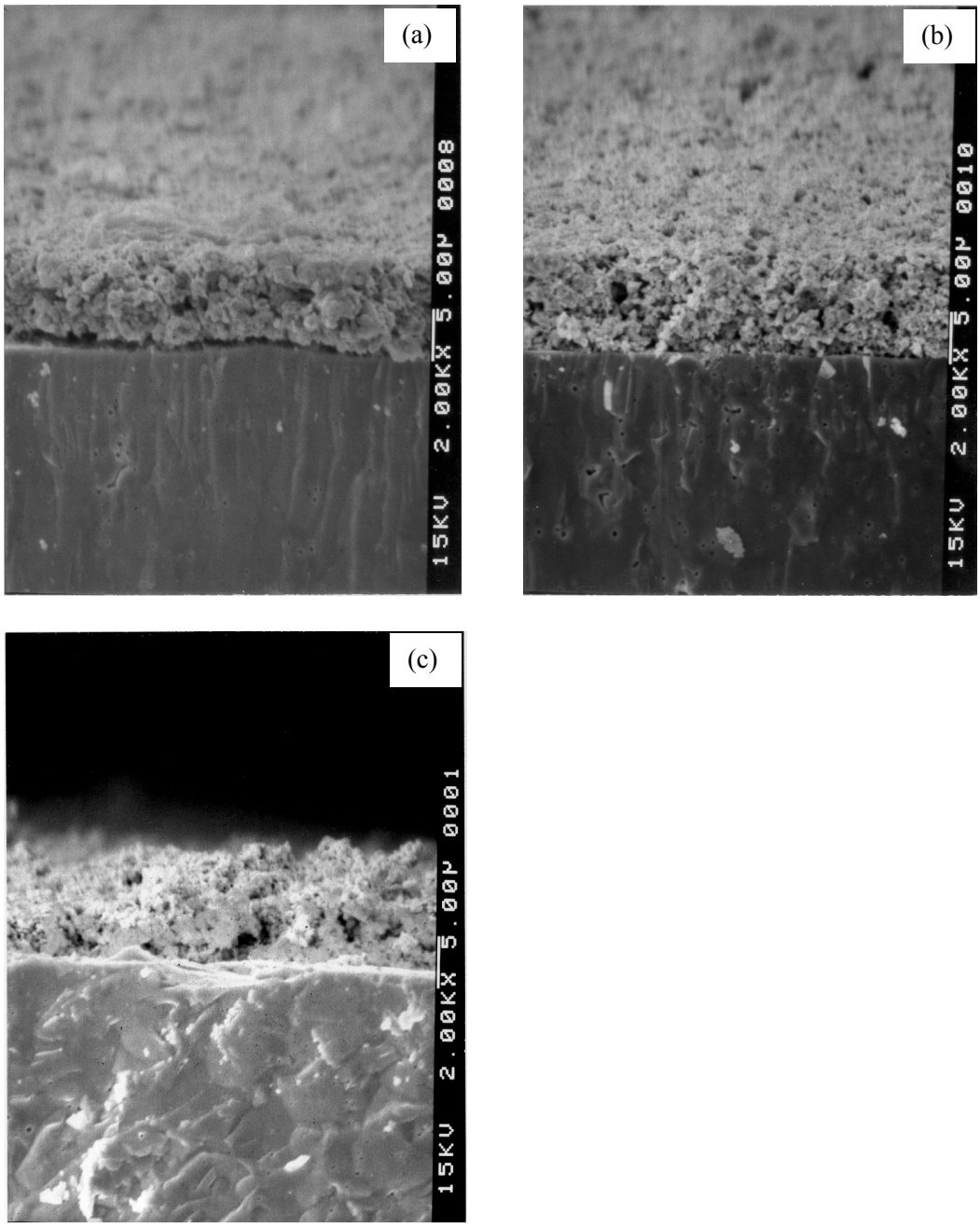

Fig. 8 SEM photographs of a cross-sectional fracture surface of LSM15-YSZ electrodes on (a) convex, (b) concave and (c) flat YSZ plates.

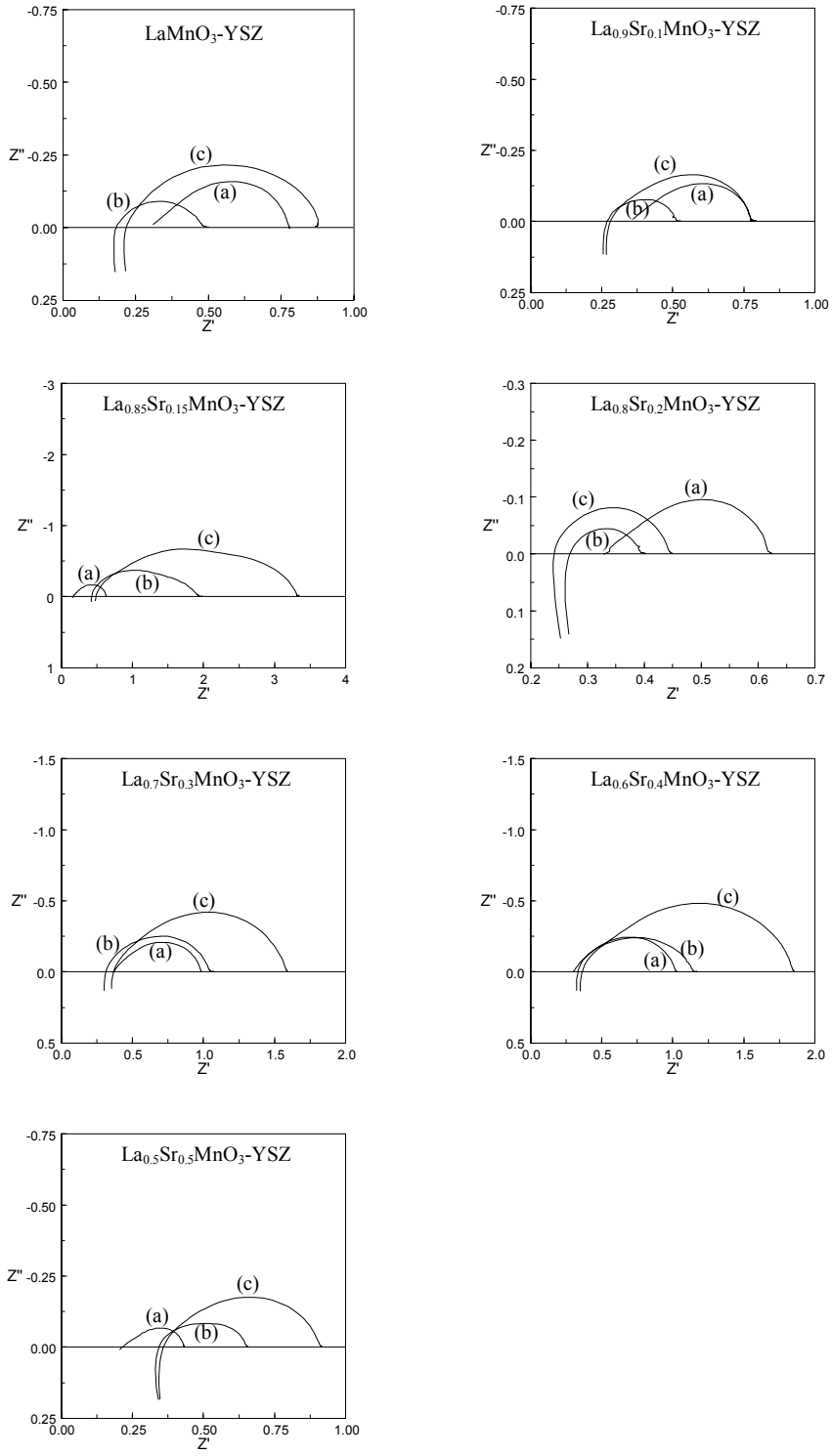

Fig. 9 Impedance spectra of LSM-YSZ cathodes before and after passing a current of 1 A / cm^2. Measurements were taken at 900°C, (a) before, (b) 4 min after and (c) 24 h after passing a current of 1 A / cm^2 for 24 h.

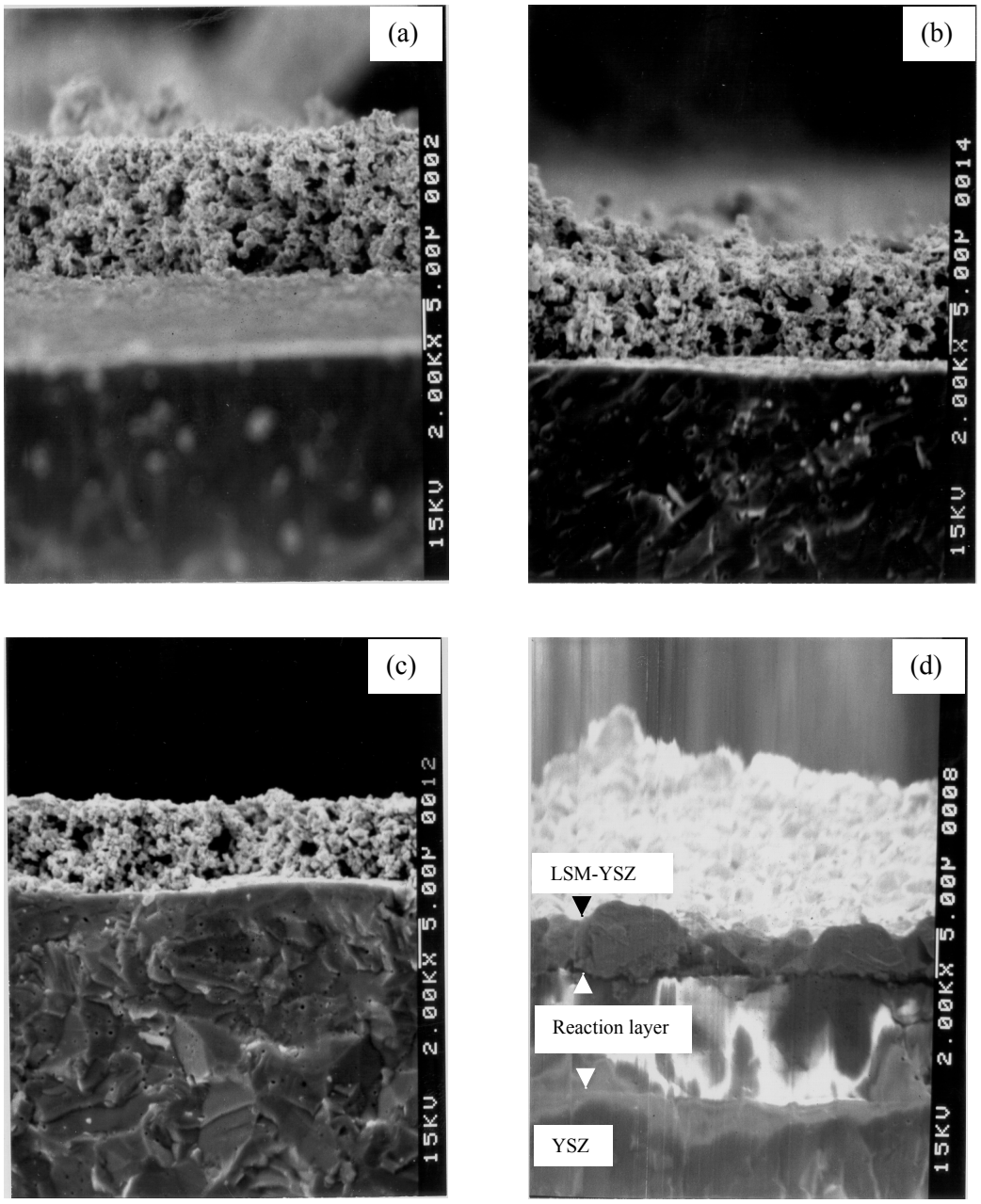

Fig. 10 SEM photographs of a cross-sectional fracture surface of LSM15-YSZ electrodes before and after current passage; (a) cathodic side before current passage, (b) anodic side before current passage, (c) cathodic side after current passage and (d) anodic side after current passage.

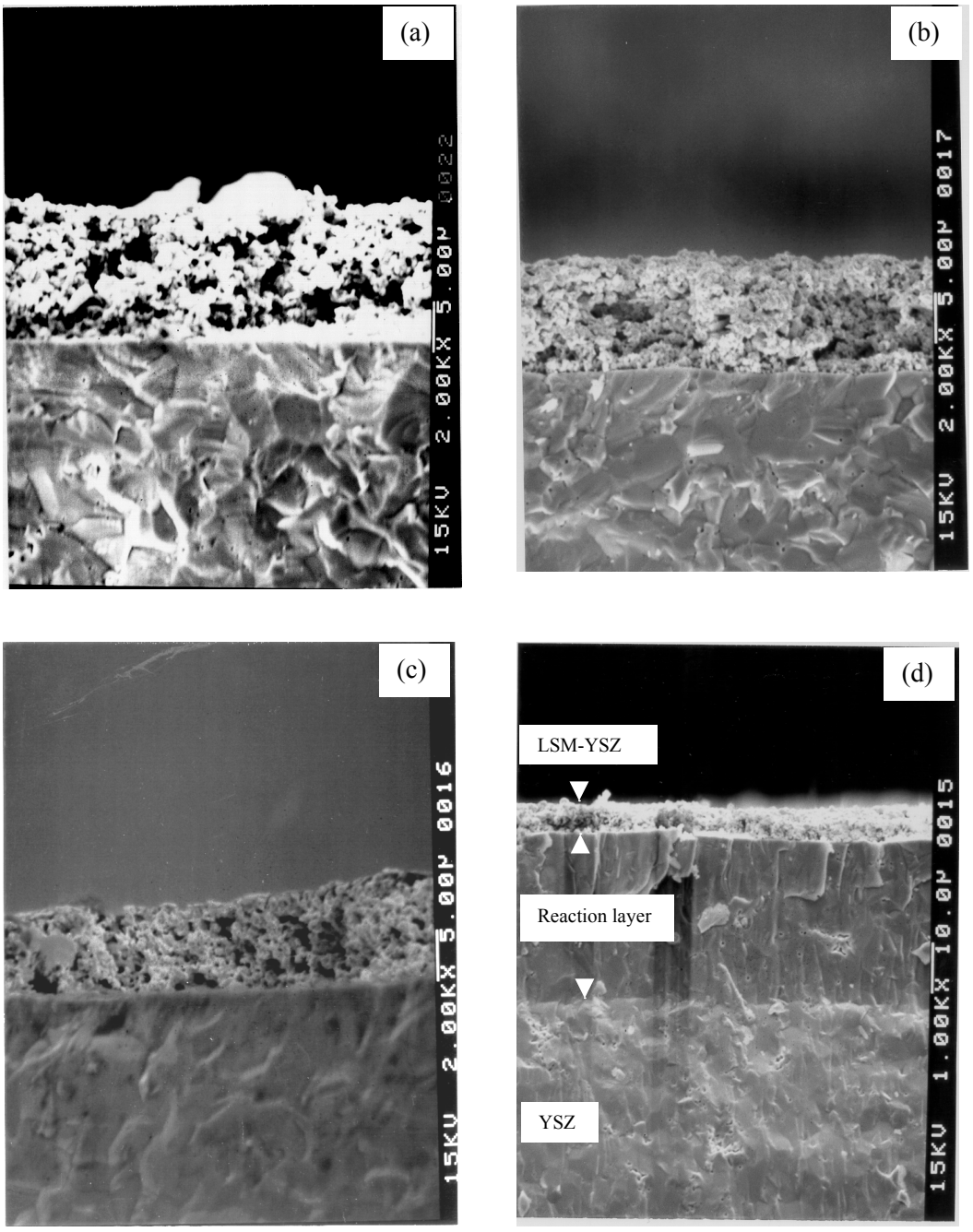

Fig. 11 SEM photographs of a cross-sectional fracture surface of LSM20-YSZ electrodes before and after current passage; (a) cathodic side before current passage, (b) anodic side before current passage, (c) cathodic side after current passage and (d) anodic side after current passage.